ELEMENT CONCENTRATION CHANGES IN MITOTICALLY ACTIVE AND POSTMITOTIC ENTEROCYTES

An X-Ray Microanalysis Study

IVAN L. CAMERON, NANCY K. R. SMITH, and THOMAS B. POOL

From the Department of Anatomy, The University of Texas Health Science Center at San Antonio, San Antonio, Texas 78284

ABSTRACT

Unfixed freeze-dried and uncoated tissue sections of the mouse duodenum were suspended across a hole in a carbon planchet and analyzed in a scanning electron microscope fitted with energy-dispersive x-ray analytical equipment. Computer analysis of the x-ray spectra allowed elemental microanalysis of the nucleus, cytoplasm, and late anaphase-early telophase chromatin regions in the cryptal and villus enterocytes. Elemental concentrations (mmol/kg dry wt) were measured for Na, Mg, P, S, Cl, K, and Ca. None of the elements were compartmentalized preferentially in either the nucleus or the cytoplasm of interphase enterocytes of crypts or in postmitotic enterocytes of villi. In contrast, Ca, S, and Cl are detectable in significantly higher concentrations in mitotic chromatin of dividing enterocytes of the crypt as compared to surrounding mitotic cytoplasm, but Na, Mg, and P are in lower concentrations in the mitotic chromatin as compared to mitotic cytoplasm. Interphase enterocytes of crypts have higher concentrations of Mg, P, and K, and lower concentrations of Na than do postmitotic enterocytes of villi.

KEY WORDS electron microprobe · mitosis · enterocytes · x-ray microanalysis · elements

This report is concerned with changes in elemental concentration in enterocytes of the duodenal epithelium as they make the transition from mitotically active cells in the progenitor compartment (in the crypts) to postmitotic enterocytes of the functional compartment (covering the villi). The report also deals with elemental redistributions between cryptal cells in interphase versus those in the late-anaphase or early-telophase stage of mitosis. We have made an important modification in our previously reported x-ray microanalysis procedures which allows greater sensitivity of elemental analysis as well as the detection of two lower atomic number elements—sodium and magnesium (3, 11). This improvement in x-ray microanalysis prompted us to reevaluate elemental concentrations in cryptal and villus enterocytes (3).

MATERIALS AND METHODS

The tissue analyzed was from a young adult female C3H mouse which had been maintained on Wayne Lab-Blox (Allied Mills, Inc., Chicago, Ill.) and water ad libitum. The animal was killed by cervical dislocation. The duodenum, 1 cm below the pyloric valve, was taken immediately and 2-mm cross sections were transected with razor blades. Tissues were prepared by the methods of Brown et al. (1). As each piece of duodenum was

J. CELL BIOLOGY © The Rockefeller University Press · 0021-9525/79/02/0444-07$1.00
Volume 80 February 1979 444-450

removed, it was attached to a tubular brass holder by using finely minced liver as an adhesive. One of the cut surfaces was placed against the liver adhesive; the other cut surface was oriented away from the liver adhesive.

The following description of tissue-section preparation and microprobe analysis is essentially the same as recently reported by Smith et al. (11): The specimen was immediately frozen by immersion in liquid propane cooled in a liquid nitrogen bath, and then transferred to a cryostat (Harris Mfg. Co., N. Billerica, Mass.) which was maintained at −30°C. After cutting into the block for a distance of 0.5–1.0 mm, 4-μm-thick sections were cut with a Minot custom microtome (Damon/IEC Div., Damon Corp., Needham Heights, Mass.). 4-μm-thick sections from within 0.5–1.0 mm of the free-cut surface of the tissue were taken to avoid analysis of sections from cut or damaged tissue surfaces. The sections were freeze-dried under vacuum for 16 h, in custom-made cryosorption glassware containing type 4A molecular sieve beads (Fisher Scientific Co., Pittsburgh, Pa.). The specimen chamber of the cryosorption apparatus was then allowed to warm to room temperature and was slowly vented to atmospheric pressure with dry nitrogen. Tissue was immediately transferred and stored in a vacuum desiccator containing calcium sulfate desiccant. For viewing and analysis, sections were placed individually across a 2-mm hole in a 1-inch-Diam carbon planchet (Earnest F. Fullam, Inc., Schenectady, N. Y.) using graphite adhesive (DAG 154, Ted Pella, Inc., Tustin, Calif.) to tack the edges. Suspending the sections in this manner minimizes the generation of x-ray continuum caused by a supporting substrate. The sections were examined without coating at 15 kV in a JEOL JSM-35 scanning electron microscope equipped with a Si(Li) x-ray detector (Nuclear Semiconductor, Inc., Mento Park, Calif.). Specimen-to-detector distance was 1.5 cm, and the takeoff angle was 40°. The data were collected, stored, and processed by a NS-880 pulse-height analysis system (Tracor Northern, Middleton, Wis.). Morphology of the specimens was recorded by photographing the secondary image from the recording cathode ray tube (CRT). For data collection, a rapid scan at × 8,000 and a selected area of 1.5 cm^2 was made for 100 s. Taking into account that the display CRT magnification was 1.5 × the actual magnification, the specimen area rastered was 1.6 μm^2.

For elemental analysis, six areas of each of the following morphological structures were analyzed: an area over the condensed chromatin of cells in the late anaphase or early telophase stage of mitosis alternated with an area of the cytoplasm in the same dividing cell; an area of the nucleus alternated with an area of cytoplasm of an interphase enterocyte in the same area as the mitotic enterocyte was measured; and an area of the nucleus alternated with an area of the cytoplasm of postmitotic enterocytes measured midway up the villus. X-ray pulse-height distribution was measured in the energy range of 0–10.22 keV with a resolution of 20 eV/channel. The Tracor Northern Super ML (multiple least squares) program was used to deconvolute the spectra and to calculate elemental peak/continuum ratios for each element in each spectrum. Chi-square values (a statistical measure of goodness of fit) for the least-squares fits ranged from 1 to 2. Continuum was arbitrarily designated as 4.50–5.00 keV, an energy interval in which no characteristic peaks were generated from the samples. For each of the seven detectable elements of biological relevance, all groups of data were subjected to the analysis of variance (ANOVA) statistical test. The continuum, which is a measure of mass, was also subjected to the ANOVA to compare mass difference. For each element a test for differences among several means (2) was used to determine which pairs of means were significantly different from each other based on a calculated critical difference between means (2).

To quantify the data further, the characteristic peak/continuum ratio for each element was compared with that of a series of standards as proposed by Hall (7). Standards were prepared by adding known weights of salts (NaCl, $MgSO_4$, KH_2PO_4, and $CaCl_2$) to bovine serum albumin (Cohn Fraction V, Sigma Chemical Co., St. Louis, Mo.). Freeze-dried 4-μm sections of the BSA solutions were prepared exactly as tissue sections were prepared. Composition of the standards was selected to approximate that of the biological specimens (20% dry solids). A series of multi-element standards was prepared in which the total weight of added electrolyte was kept nearly constant in all albumin standards by adjusting the relative amounts of the various salts. Such adjustments were not practical in the calcium standards because of the insolubility of calcium salts in the multi-element matrices. Thus a separate set of standards were prepared for calcium using $CaCl_2$ and BSA. Freeze-dried albumin sections of four different concentrations for each element, covering the range from 35 to 700 mmol/kg dry weight, were microprobed. A section prepared from 20% BSA with no electrolytes added was also probed to serve as a blank. Elemental peak/continuum values for the BSA standards were corrected for the amounts of the individual elements present in the blank (specifically Na, S, and Cl). The peak/continuum-concentration data for each element were subjected to a least-squares linear-regression analysis.

RESULTS

Fig. 1 shows a scanning electron micrograph (secondary electron image) of a 4-μm thick freeze-dried section of mouse duodenal crypts photographed under conditions used for x-ray microanalysis. Visible are nuclei and cytoplasm of cryptal cells and mitotic cells. The morphology of the tissue is entirely adequate for selection of discrete areas of nucleus, cytoplasm, or mitotic chromatin for microprobe analysis. Three types of evidence

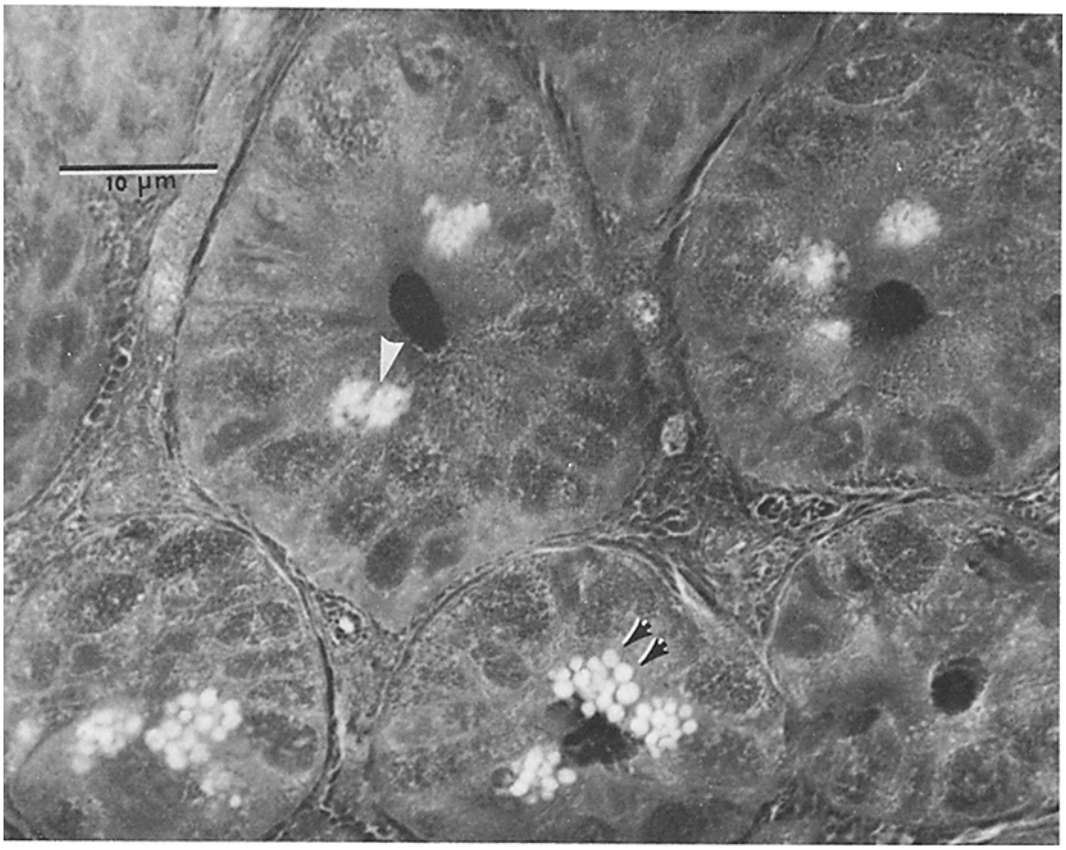

FIGURE 1 Scanning electron micrograph (secondary electron image) of freeze-dried, uncoated 4-µm cross section of duodenal crypts. The lumena of the crypts are clearly visible as are the nucleus and cytoplasm of interphase enterocytes. The white arrowhead points to a late-anaphase mitotic figure near the crypt lumen. The double arrowheads point to granules in Paneth cells towards the bottom of the crypts. × 1,975.

were used to verify our ability to distinguish mitotic chromatin from other cell areas such as the Paneth cell granules, which are seen in Fig. 1. First, the freeze-dried sections used for microprobe analysis were stained with acetocarmine (which does not stain Paneth granules) (see Fig. 2). Such stained sections revealed the late anaphase to early telophase figures seen in the secondary electron image to be the same structures. Second, x-ray energy dispersive spectra were collected from Paneth cell granules and were compared to mitotic chromatin spectra (listed in Table I). A Student's *t* test was run for the mean concentration of each element. The mean element concentrations (mmol/kg dry weight) for the granules plus the probability of difference from mitotic chromatin (in parentheses) are as follows: Na = 150.2 ± 21.0 (not significant), Mg = 16.43 ± 6.9 (<0.01), P = 236.1 ± 27.6 (< 0.05), S = 408.1 ± 40.4 (not significant), Cl = 192.6 ± 22.2 (<0.001), K = 208.6 ± 21.7 (<0.001), and Ca = 151.3 ± 11.7 (<0.001). Thus, five of the seven elements show significant differences in element concentration. This again indicates that we have measured element concentrations in two morphologically distinct structures. Finally, the strongest evidence for our ability to distinguish such structures comes from the fact that a measurable amount of zinc was detected in every x-ray spectrum from a Paneth granule, but zinc was never detected in spectra collected from mitotic chromatin or the other areas measured.

The derived least-squares linear regression calibration curves for peak/continuum versus concen-

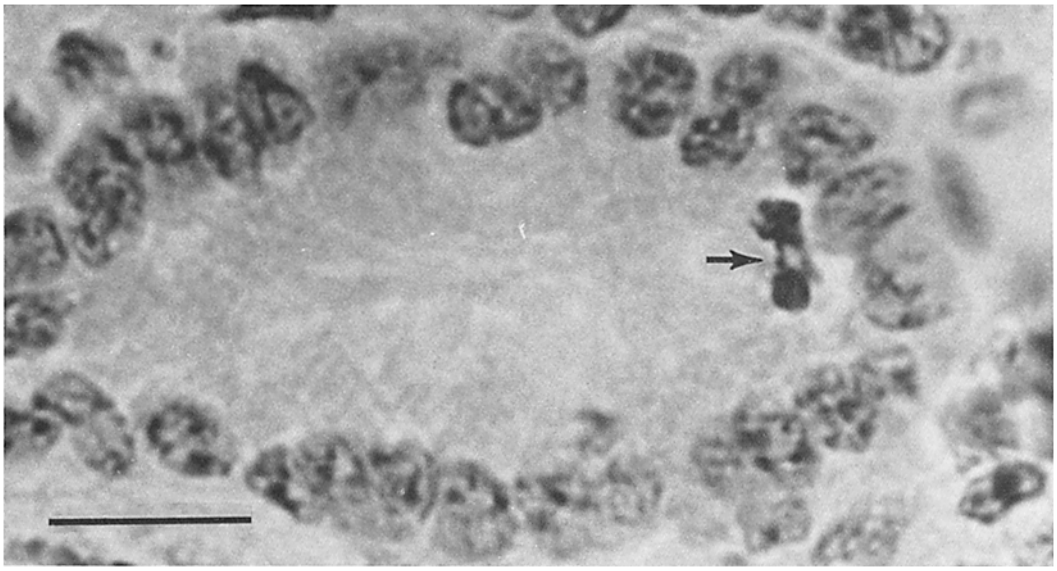

FIGURE 2 Micrograph of a freeze-dried section previously used for microprobe analysis. This section was stained with acetocarmine (which does not stain Paneth granules). Comparison of such stained sections after secondary-electron imaging helps verify our ability to recognize mitotic chromatin by the secondary electron image. × 2,423. Bar, 10 μm.

tration for Na, Mg, P, S, Cl, K, and Ca in the 4-μm freeze-dried BSA standards are shown in Fig. 3. As predicted by the Hall theory (7), which has recently been rigorously tested and validated for biological thin sections by Shuman et al. (9), linear calibration curves were obtained for all elements. As pointed out by Dorge et al. (4), the use of albumin standards with similar composition to the biological specimen avoids the problem of corrections for differences in mean atomic number and simplifies the quantification procedure. Based on the calibration curves, a constant of proportionality was obtained for each element and was used to convert peak/continuum data to mmol/kg dry weight. Table I summarizes the elemental concentrations for the tissue areas analyzed.

Included in Table I are the results of the one-way analyses of variance for the data on each element. Analysis of the concentration of elements can be sorted into three main categories: (*a*) the distribution of elements between the nucleus and the cytoplasm of cryptal or of villus enterocytes; (*b*) the redistribution of elements at the late anaphase-early telophase stage of mitosis; and (*c*) the differences in element concentration between the mitotically active cryptal cells and the postmitotically active villus cells.

Our data (Table I) show no significant nuclear-cytoplasmic compartmentalization of any element in either the interphase cell in the crypts or the postmitotic villus enterocyte. Thus, the average nuclear/cytoplasmic (n/c) ratio is almost unity for each element and does not change during the transition from the mitotically active interphase enterocyte to the postmitotic enterocyte.

The data in Table I show several significant differences between the interphase nucleus and cytoplasm and the chromatin of late anaphase-early telophase stage of mitosis in the cryptal progenitor cells. Ca, S, and Cl are all significantly concentrated in mitotic chromatin as compared to the cytoplasm of the same cell, or to the cytoplasm or nucleus of the progenitor cell, in interphase. Cl and S are concentrated ~two-fold in the mitotic chromatin, while Ca is concentrated from ~2.5- to 8-fold. Conversely, the mitotic chromatin has lower concentrations of Na, Mg, and P than cytoplasm.

The interphase cells of the progenitor compartment reveal a significantly higher concentration of Mg, P, and K and significantly lower concentrations of Na compared to the postmitotic villus cells (Table I).

DISCUSSION

The quick-freezing procedures we have used have

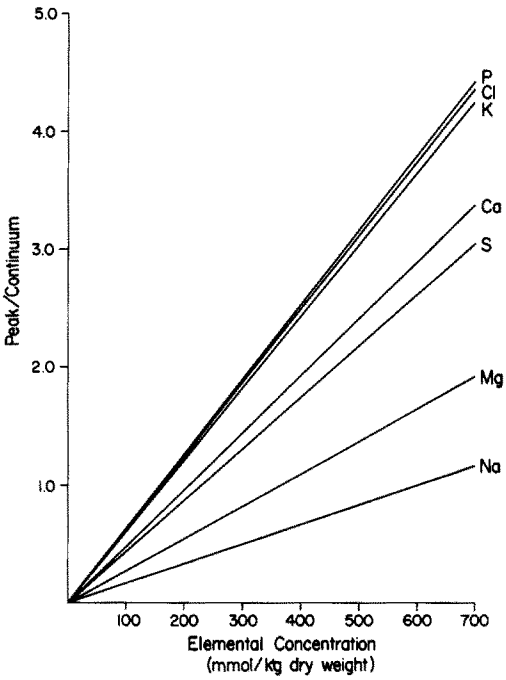

FIGURE 3 Calibration curves for Na, Mg, P, S, Cl, and Ca obtained on freeze-dried 4-μm sections of 20% albumin with known electrolyte content. Each curve is the derived least-squares linear-regression fit of the data for a particular element, with corrected peak/continuum values for the BSA blank.

been developed and rigorously tested by others (1, 12, 13) and have been shown not to redistribute soluble or diffusible substances. Our sectioning temperature of −30°C is above the recrystallization temperature of ice, and cutting at this temperature would not be recommended for high spatial resolution electron-probe microanalysis of small subcellular organelles. The ice crystal distortions seen in Fig. 1 are certainly responsible for some redistribution of elements, at least to the extent of the dimensions of the ice crystals. Our preparative method does indeed allow some redistribution of mass to occur at the dimensions of the ice crystals formed (Pool et al., unpublished observations). However, ice crystal formation does not create elemental gradients or redistribute any element preferentially (as measured in the albumin standards) unless the area beamed is totally within the boundaries of a single ice crystal reticulation. The size of these ice crystal reticulations therefore determines the minimum analytical spatial resolution obtained by our preparative methods. The analyzed area (1.6 μm^2) was larger than 99% of the ice crystal reticulations measured in our tissue specimens. Thus, on the basis of the lack of diffusion of soluble material (cited above) and our own studies, we feel safe in assuming that no major translocations of elements have occurred at the level of structures at which we are working (i.e., resolution of cytoplasmic, nuclear, or mitotic chromatin areas) for microprobe analysis.

The elevated levels of Ca, S, and Cl in mitotic chromatin of cryptal enterocytes seen in this study confirm the results included in a previous report from our laboratory (3). The methods we now employ to reduce continuum x-ray counts from nonbiological sources have enabled us to show that P, Mg, and Na are present in significantly lower concentrations in the mitotic chromatin as compared to mitotic cytoplasm or interphase enterocytes. Several of the elemental redistributions in mitotic chromatin, as detected by x-ray microanalysis, correspond to chemical modifications of nuclear macromolecules during cell division as seen by other methods. Gurley et al. (5, 6) have shown that there is a striking dephosphorylation of some chromosomal proteins at late anaphase-early telophase. It is during this period of the division cycle that we have detected a significant depression in chromatin P levels with microprobe analysis. Further, the significant increase in S concentration in mitotic chromatin which we have observed at this same stage corresponds to a time when sulfhydral proteins are high in mitotic chromatin. Kawamura and Dan (8) have used elegant methods to visualize sulfhydral-containing regions in the mitotic apparatus and have shown that the cytochemical reactivity of these groups increases until the nuclear reconstruction stage after mitosis. The reason for lower concentrations of Mg and Na and higher concentrations of Ca in chromatin during late anaphase-early telophase is not known. Clearly, Mg and Ca play important roles in both microtubule assembly and disassembly as well as in function of the mitotic apparatus.

Our findings of changes in elemental concentrations between mitotically active cryptal cells and postmitotic villus cells indicate that a major transition in a cell's functional state can be accompanied by significant changes in the elemental composition of both nucleus and cytoplasm. At the present time, it is not known if the specific changes in elements of villus cells (lower Mg, P, and K; higher Na) relate to the loss of the cells' proliferative potential, or if they reflect the acquisition of

TABLE I

Element Concentration (mmol/kg dry weight) for Analyzed Areas of Duodenal Enterocytes

Area analyzed	Sodium	Magnesium	Phosphorus	Calcium
Mitotic chromatin, crypt cell	138.9 ± 6.0	45.6 ± 7.2	298.5 ± 17.3	87.1 ± 6.2
Cytoplasm, crypt cell	188.3 ± 12.0	64.4 ± 7.2	674.6 ± 42.4	35.8 ± 6.2
Nucleus, interphase crypt cell	240.2 ± 12.0	66.6 ± 3.6	761.0 ± 23.6	10.7 ± 2.1
Cytoplasm, interphase crypt cell	219.3 ± 6.0	68.8 ± 3.6	726.1 ± 28.3	14.2 ± 2.1
Nucleus, villus cell	298.6 ± 47.7	39.8 ± 3.6	571.2 ± 37.7	8.2 ± 2.1
Cytoplasm, villus cell	322.4 ± 47.7	43.4 ± 3.6	547.0 ± 59.7	12.4 ± 4.1
Statistical analysis				
F value	5.52*	6.28‡	20.37‡	38.53‡
CDBM§	83.4 (0.05)	15.2 (0.05)	107.2 (0.05)	15.2 (0.05)
	112.1 (0.01)	20.3 (0.01)	144.0 (0.01)	20.6 (0.01)
	147.8 (0.001)	26.8 (0.001)	190.0 (0.001)	27.2 (0.001)

Area analyzed	Sulfur	Chlorine	Potassium	Continuum
Mitotic chromatin, crypt cell	516.2 ± 18.3	357.8 ± 14.4	569.4 ± 11.5	9131 ± 277
Cytoplasm, crypt cell	249.4 ± 20.6	230.7 ± 11.2	560.4 ± 6.6	5556 ± 258
Nucleus, interphase crypt cell	235.4 ± 13.7	195.0 ± 3.2	567.8 ± 21.3	4810 ± 514
Cytoplasm, interphase crypt cell	214.3 ± 6.9	195.8 ± 6.4	553.7 ± 9.8	5513 ± 583
Nucleus, villus cell	205.2 ± 2.3	215.4 ± 17.6	399.7 ± 22.9	5711 ± 156
Cytoplasm, villus cell	203.1 ± 16.0	218.6 ± 14.4	377.0 ± 21.3	6701 ± 301
Statistical analysis				
F value	70.98‡	25.04‡	30.48‡	16.51‡
CDBM§	41.5 (0.05)	35.2 (0.05)	47.2 (0.05)	1090 (0.05)
	55.7 (0.01)	47.4 (0.01)	63.3 (0.01)	1463 (0.01)
	73.5 (0.001)	62.4 (0.001)	83.5 (0.001)	1931 (0.001)

Tissue was taken in 2-mm cubes from the duodenum of a mouse. After rapid freezing in liquid propane, 4-μm sections were prepared. Using an accelerating voltage of 15 kV, elemental x-ray data were collected for 100 s from uncoated, freeze-dried sections mounted on carbon planchets. Ratios given are the means ± SE for six cells from each area.

* Significant *F* value ($P < 0.02$).

‡ Significant *F* value ($P < 0.001$).

§ Critical differences between means in each column. Means in each column which differ by these values are significantly different at the indicated level of probability (in parentheses).

‖ Continuum is determined from total x-ray counts generated from the Bremsstrahlung continuum (4.5–5.0 keV).

the cells' specific function (absorption) as the enterocyte moves from the progenitor compartment to the functional compartment of the duodenum.

Significant differences in elemental concentrations were not detected between the nuclear and cytoplasmic compartments of interphase enterocytes of the crypt or of the villus. This, however, does not appear to be true for all interphase cells, nor does it reflect a cell's potential to divide. We have recently studied the nuclear-cytoplasmic distribution of elements in normal and cancerous liver cells by using the same procedures as were used in this study (11). Normal interphase hepatocytes have more Cl in the cytoplasm than in the nucleus whereas interphase hepatoma cells have more Cl in the nucleus than in the cytoplasm. Additionally, S is slightly (but significantly) concentrated in the nucleus of interphase hepatocytes but is not compartmentalized in hepatoma cells. Although earlier studies have reported larger concentration differences of elements between the

nucleus and cytoplasm of hepatocytes (10), our rapid-freezing procedures allow us to detect elemental concentrations as they exist *in situ*. To our knowledge, this is not possible with any other method. Currently, we are using these techniques to investigate the possibility that certain elemental distributions are characteristic of (*a*) mitotically active cells; (*b*) nonproliferating cells that are still capable of being recruited back into the dividing population (G_0); and (*c*) postmitotic, terminally differentiated cells that apparently cannot be induced to divide.

In general, such quantitative information on elemental distributions and redistributions associated with various cellular processes, such as mitosis, cell reproduction, and so forth, will lead us to universal patterns, principles, testable predictions, and even to new therapeutic approaches in the field of cell biology.

This work was supported by United States Public Health Service grant CA16831 from The National Cancer Institute (I. L. Cameron) and by a National Institutes of Health institutional grant SO1 RR05654 (N. K. R. Smith).

Received for publication 30 January 1978, and in revised form 10 October 1978.

REFERENCES

1. Brown, D. A., W. E. Stumpf, and L. J. Roth. 1969. Localization of radioactive labelled extracellular fluid indicators in nervous tissue by autoradiography. *J. Cell Sci.* **4**:265–288.
2. Bruning, J. L., and B. L. Kintz. 1968. Computational Handbook of Statistics. Scott, Foresman & Company, Glenview, Ill. 112–114.
3. Cameron, I. L., R. L. Sparks, K. L. Horn, and N. R. Smith. 1977. Concentration of elements in mitotic chromatin as measured by x-ray microanalysis. *J. Cell Biol.* **73**:193–199.
4. Dorge, A., R. Rick, K. Gehring, and K. Thurau. 1978. Preparation of freeze-dried cryosections for quantitative X-ray microanalysis of electrolytes in biological soft tissues. *Pfluegers Archiv Eur. J. Physiol.* **373**:85–97.
5. Gurley, L. R., R. A. Walters, and R. A. Tobey. 1974. Cell cycle-specific changes in histone phosphorylation associated with cell proliferation and chromosome condensation. *J. Cell Biol.* **60**:356–364.
6. Gurley, L. R., R. A. Walters, and R. A. Tobey. 1978. Histone phosphorylation and chromatin structure in synchronized mammalian cells. *In* Cell Cycle Regulation. J. R. Jeter, I. L. Cameron, G. M. Padilla, and A. M. Zimmerman, editors. Academic Press, Inc., New York. 37–60.
7. Hall, T. A. 1971. The microprobe assay of chemical elements. *Phys. Tech. Biol. Res.* **IA**:151–267.
8. Kawamura, N., and K. Dan. 1958. A cytochemical study of the sulfhydryl groups of sea urchin eggs during the first cleavage. *J. Biophys. Biochem. Cytol.* **4**:615–619.
9. Shuman, H., A. V. Somlyo, and A. P. Somlyo. 1976. Quantitative electron probe microanalysis of biological thin sections: methods and validity. *Ultramicroscopy.* **1**:317–339.
10. Siebert, G. 1972. The biochemical environment of the mammalian nucleus. *Sub-Cell. Biochem.* **1**:277–292.
11. Smith, N. R., R. L. Sparks, T. B. Pool, and I. L. Cameron. 1978. Differences in intracellular concentration of elements in normal and cancerous liver cells. An x-ray microanalysis study. *Cancer Res.* **38**: 1952–1959.
12. Stumpf, W. E., and L. J. Roth. 1966. High resolution autoradiography with dry-mounting, freeze-dried frozen sections. *J. Histochem. Cytochem.* **14**:274–287.
13. Stumpf, W. E., and L. J. Roth. 1969. Autoradiography using dry-mounted freeze-dried sections. *In* Autoradiography of Diffusible Substances. L. J. Roth and W. E. Stumpf, editors. Academic Press, Inc., New York. 69–80.